The dynamics of Saturn's main aurorae

A. Bader[1], S. V. Badman[1], S. W. H. Cowley[2], Z. H. Yao[3], L. C. Ray[1], J. Kinrade[1], E. J. Bunce[2], G. Provan[2], T. J. Bradley[2], C. Tao[4,5], G. J. Hunt[6], W. R. Pryor[7]

[1]Department of Physics, Lancaster University, Lancaster, UK
[2]Department of Physics and Astronomy, University of Leicester, Leicester, UK
[3]Laboratoire de Physique Atmosphérique et Planétaire, Space sciences, Technologies and Astrophysics Research (STAR) Institute, Université de Liège, Liège, Belgium
[4]National Institute of Information and Communications Technology, Koganei, Japan
[5]Department of Geophysics, Tohoku University, Sendai, Japan
[6]Blackett Laboratory, Imperial College London, London, UK
[7]Science Department, Central Arizona College, Coolidge, Arizona, USA

Key Points:

- A dawn-dusk asymmetry in Saturn's auroral emissions due to Dungey cycle activity is not observed under typical solar wind driving
- The previously observed statistical intensity maximum at dawn is the result of large-scale auroral plasma injections from Saturn's nightside
- The phasing of these auroral injections indicates that magnetotail reconnection seems to partly be governed by planetary period oscillations

Corresponding author: Alexander Bader, a.bader@lancaster.ac.uk

Abstract

Saturn's main aurorae are thought to be generated by plasma flow shears associated with a gradient in angular plasma velocity in the outer magnetosphere. Dungey cycle convection across the polar cap, in combination with rotational flow, may maximize (minimize) this flow shear at dawn (dusk) under strong solar wind driving. Using Cassini-UVIS imagery, we surprisingly find no related asymmetry in auroral power but demonstrate that the previously observed "dawn arc" is a signature of quasiperiodic auroral plasma injections commencing near dawn, which seem to be transient signatures of magnetotail reconnection and not part of the static main aurorae. We conclude that direct Dungey cycle driving in Saturn's magnetosphere is small compared to internal driving under usual conditions. Saturn's large-scale auroral dynamics hence seem predominantly controlled by internal plasma loading, with plasma release in the magnetotail being triggered both internally through planetary period oscillation effects and externally through solar wind compressions.

Plain language summary

Saturn's main aurorae are thought to be generated as a result of sheared plasma flows near the boundary between the rapidly rotating magnetosphere of Saturn and interplanetary space. It is often assumed that the steady flow of the solar wind away from the Sun has an impact on this flow shear; due to the direction of Saturn's rotation the aurorae would then have to be brighter at the planet's dawn side than on its dusk side, which was observed in previous studies. Here we analyze a large set of auroral images taken by Cassini's ultraviolet camera, but we cannot find any sign of such an asymmetry. This indicates that the impact of the solar wind on Saturn's aurorae must be smaller than previously thought, and that Saturn's aurorae must instead mainly be controlled from within the system. This assumption is supported by our observations of bright auroral patches at dawn, which are likely a signature of plasma being released from Saturn's magnetosphere and appear at quite regular periods corresponding to Saturn's rotation period.

1 Introduction

Planetary aurorae appear throughout the solar system and illustrate many different plasma processes. Their origins are very different - while, e.g., aurorae on Earth and Mars are almost entirely controlled by the solar wind (e.g., Brain et al., 2006; Milan et al., 2003; Walach et al., 2017), Jupiter's brightest aurorae are internally generated due to the breakdown of corotation in the middle magnetosphere (e.g., Cowley & Bunce, 2001; Hill, 2001; Southwood & Kivelson, 2001). While also being a fast-rotating gas giant like Jupiter, Saturn's corotation breakdown currents are thought too weak to produce auroral emissions (Cowley & Bunce, 2003). Instead, the flow shear associated with a strong gradient in angular plasma velocity between the outer closed magnetosphere and the open field region - caused by ion-neutral collisions in the ionosphere twisting the open field lines (Isbell, Dessler, & Waite, 1984; Milan, Bunce, Cowley, & Jackman, 2005) - was proposed as a possible driver generating the field-aligned currents (FACs) responsible for electron precipitation into Saturn's polar atmosphere, forming the "subcorotational system" (e.g., Cowley et al., 2005; Cowley, Bunce, & O'Rourke, 2004; Cowley, Bunce, & Prangé, 2004; Stallard et al., 2007; Vasyliūnas, 2016).

Under strong solar wind driving (increased solar wind velocity and density), active Dungey cycle reconnection between the interplanetary magnetic field and Saturn's magnetic field at the dayside magnetopause may prompt an antisunward flow in the slowly subcorotating polar open field region just like at Earth (Dungey, 1961). At dawn, this Dungey cycle convection across the polar cap - here oppositely directed to the subcorotating magnetospheric plasma flow - would act to enhance the (rotational) plasma flow shear associated with the generation of Saturn's main aurorae and hence also the auroral brightness. Conversely, strong solar wind driving should lead to a reduction of this plasma flow shear and the auroral brightness at dusk (e.g., Cowley, Bunce, & Prangé, 2004; Jackman & Cowley, 2006). Adding to this local time (LT) asymmetry, the Dungey and Vasyliunas cycle return flows are expected to pass from the magnetotail toward the dayside via dawn due to the rapid rotation of the magnetosphere (e.g., Cowley, Bunce, & Prangé, 2004; Vasyliūnas, 1983). However, the importance of Dungey-cycle convection at Saturn is disputed as magnetopause reconnection may be inhibited across parts of the magnetopause (e.g., Desroche, Bagenal, Delamere, & Erkaev, 2013; Masters et al., 2012, 2014) and viscous interactions mediated by Kelvin-Helmholtz instabilities may instead be the main coupling mechanism between the solar wind and Saturn's magnetosphere (e.g., Delamere & Bagenal, 2010; Delamere, Wilson, Eriksson, & Bagenal, 2013).

Previous studies using auroral imagery obtained by the Hubble Space Telescope in the ultraviolet (UV) wavelength band (e.g., Kinrade et al., 2018; Lamy et al., 2009, 2018; Nichols et al., 2016) and by the Cassini spacecraft at infrared (IR) and UV wavelengths (e.g., Bader et al., 2018; Badman et al., 2011; Carbary, 2012) have statistically identified such a brightness asymmetry, seemingly confirming that Saturn's main aurorae are indeed significantly solar wind-driven. However, most of these studies used rather small sets of single exposures lacking context and/or short observation series without good time resolution to obtain statistical averages, hence not taking into account the complicated dynamics of Saturn's aurora which had already been observed by the Voyager spacecraft (Sandel & Broadfoot, 1981; Sandel et al., 1982).

In this study we use extensive sets of auroral imagery obtained by the Cassini spacecraft to investigate the dynamics of Saturn's main aurorae and shed more light on its generation mechanisms. We present the dataset and describe our analysis methods in section 2. In section 3 we analyze observations consistent with quiet auroral conditions to reveal the structure of subcorotationally driven main aurorae and their modulation by planetary period oscillations (PPOs), while in section 4 we describe the added complexity brought into the system by magnetotail dynamics, causing transient large-scale brightenings. We summarize our findings and propose an updated model of Saturn's main aurorae in section 5.

2 Data and methods

NASA's Cassini spacecraft orbited Saturn for over 13 years, providing a rich set of auroral observations in the UV spectrum with its Ultraviolet Imaging Spectrograph (UVIS, Esposito et al. (2004)). Here we investigate Saturn's auroral dynamics, and therefore select observation windows where many images were taken in quick succession (exposure time < 20 min) for several hours. This corresponds to auroral observations from high apoapsis where Cassini moved relatively slowly, preserving the same viewing geometry for long periods; and where the large distance from Saturn allowed UVIS to cover the entire auroral oval with a single slit scan, allowing for low exposure times. Nearly all available observations of this kind fall into 2014/2016/2017, and all are from Saturn's northern hemisphere.

2.1 Cassini-UVIS imagery

The Cassini-UVIS instrument includes two telescope-spectrographs observing in the 56−118 nm (extreme ultraviolet, or EUV) and 110−190 nm (far ultraviolet, or FUV) wavelength ranges; most of Saturn's auroral UV emissions are observed in the FUV band. The UVIS FUV slit has a field of view of 1.5×64 mrad, with 64 spatial pixels of size 1.5×1 mrad each arranged along a single line. Pseudo-images of the aurora are obtained by scanning this slit across the auroral region. Several successive scans may be necessary to cover the entire region of interest depending on Cassini's distance from Saturn, increasing the exposure time of auroral images. The total exposure time for a pseudo-image of the entire auroral oval can vary between $6 - 180\,\mathrm{min}$.

Each image is polar projected onto a planetocentric polar grid with resolution $0.5° \times 0.25°$ (lon $\times$ lat) at an altitude of 1100 km above Saturn's 1 bar pressure surface (oblate spheroid with $R_{\mathrm{SEQ}} = 60268\,\mathrm{km}$ and $R_{\mathrm{SPO}} = 54364\,\mathrm{km}$ as equatorial and polar radii), the approximate altitude of Saturn's auroral emissions (Gérard et al., 2009). Cassini SPICE pointing information is used to perform the projection. The spectrum recorded by each pixel of the UVIS FUV sensor, observed in 1024 spectral bins, is reduced to total unabsorbed H_2 emission intensity ($70-170\,\mathrm{nm}$) by multiplying the intensity measured in the $155-162\,\mathrm{nm}$ range by the factor 8.1 (Gustin et al., 2017, 2016). Using this method, dayglow emission and hydrocarbon absorption affect the estimated total unabsorbed H_2 intensity as little as possible. Even so, some dayglow is still apparent in most UVIS images; it is removed as previously described in Bader, Badman, Yao, Kinrade, and Pryor (2019) in order to obtain accurate auroral brightnesses and emission powers.

Many of the images in this study have quite low spatial resolutions, with single pixels extending over up to 5° in colatitude or 1 h in LT. However, this issue is circumvented by integrating over the auroral brightness to obtain the emitted radiant flux, or "auroral power", as laid out in the Supporting Information of this paper. A large instrument pixel covering a small bright auroral feature and its surroundings is dimmer than the actual brightness maximum of the observed emission - however, the pixel brightness corresponds to the average brightness of the area it subtends during the time of the exposure. Integrating over this area therefore gives a quite exact measure of the auroral power nevertheless. We reduce each image by integrating its auroral brightness between $8 - 22°$ colatitude in 36 LT bins and thereby obtain a distribution of auroral power per hour of LT. This latitudinal range fully includes the statistical position of the main aurorae and associated uncertainties (Bader, Badman, Kinrade, et al., 2019). Arranging these integrated powers of all images along the horizontal axis - taking into account the start and stop times of each exposure - we obtain a keogram.

2.2 Planetary period oscillation systems

Each of Saturn's hemispheres is associated with one PPO system, a complex array of FACs spanning the entire magnetosphere of Saturn (e.g., Andrews, Coates, et al., 2010; Hunt et al., 2014; Provan et al., 2011; Southwood & Kivelson, 2007) likely associated with vortical flow structures in Saturn's polar ionospheres (e.g., Hunt et al., 2014; Jia & Kivelson, 2012; Jia, Kivelson, & Gombosi, 2012; Southwood & Cowley, 2014). Their rotation at roughly the planetary period generates periodic signatures in all plasma properties and processes in Saturn's environment, the two systems exhibiting close but distinct periods which vary with time (e.g., Provan et al., 2016; Provan, Cowley, Sandhu, Andrews, & Dougherty, 2013). Each PPO system is usually dominant in one hemisphere, but its associated system of FACs partly closes in the opposite hemisphere such that each hemisphere experiences a double modulation of, e.g., auroral FACs by both the northern and southern PPO systems (e.g., Bader et al., 2018; Bradley, Cowley, Provan, et al., 2018; Hunt et al., 2015; Provan et al., 2018).

A sketch of the northern PPO system is shown in Supporting Figure S1, with S1a showing the magnetic field and electric currents in the equatorial plane and S1b showing the electric currents and atmospheric/ionospheric flows in the northern polar ionosphere. The southern PPO system effects the same pattern of upward/downward FACs in the northern hemisphere as shown here for the northern system. Depending on the relative orientation between the two systems, their associated FACs can combine to intensify or negate one another. The orientation of the two PPO systems is described by the PPO phase angles $\Phi_{\mathrm{N,S}}$, the counterclockwise azimuthal angle between the PPO magnetic perturbation dipoles in the equatorial plane and local noon. In this study we use the phase angles determined by Provan et al. (2018, 2016). PPO-fixed reference frames are defined using the phase values $\Psi_{N,S}$, giving the clockwise angle from the PPO dipole direction.

In the northern hemisphere, the PPO-associated upward FACs maximize at $\Psi_{N,S} = 90°$, with the downward FACs maximizing at $\Psi_{N,S} = 270°$ (e.g., Bader et al., 2018; Hunt et al., 2014). The modulation effect is hence largest when the two PPO systems are in phase, their perturbation dipoles parallel. In the keograms shown through this study and in the Supporting Information, $\Psi_{N,S} = 90°$ is marked with yellow lines.

The PPO-induced modulation of the equatorial current sheet shows a different phasing; the current sheet being thinnest at $\Psi_N = 0°$ and $\Psi_S = 180°$ (Bradley, Cowley, Bunce, et al., 2018; Cowley & Provan, 2017; Jackman, Provan, & Cowley, 2016). This modulation is therefore emphasized when the two PPO systems are in antiphase. In Figure 4 and Supporting Figure S4, the two systems were within 45° of antiphase - orange-dotted lines hence indicate the approximate location at which the PPO-related thinning of the current sheet is expected to be most pronounced.

3 Saturn's quiet main aurora - subcorotational and PPO systems

In quiet and steady auroral conditions, the main aurorae should form a quasistatic ring of emission around both poles corresponding to the region of peak flow shear between the rapidly rotating magnetospheric plasma and the slowly rotating plasma in the polar open field region (e.g., Cowley et al., 2005; Cowley, Bunce, & O'Rourke, 2004; Cowley, Bunce, & Prangé, 2004; Stallard et al., 2007; Vasyliūnas, 2016). Lacking continuous upstream solar wind monitoring, we cannot know for sure the solar wind conditions during most of Cassini's observation sequences. We therefore identify "quiet conditions" as imaging sequences where no large-scale transient brightenings (total power > 20 GW for > 5 h) were observed, indicating low magnetic reconnection activity at both dayside and nightside as such events would manifest as bifurcations at noon-dusk LTs (e.g., Badman et al., 2013; Meredith, Alexeev, et al., 2014; Radioti et al., 2013, 2011) or as bright transient features at midnight-dawn LTs (e.g., Jackman et al., 2013; Lamy et al., 2013). Figure 1 shows an auroral keogram of one such period without transient events, covering more than two full Saturn rotations (~ 25 h) with near-continuous imagery.

We notice a periodic modulation of the emitted UV auroral power, which is well explained with rotating patterns of upward and downward FACs associated with Saturn's PPO systems. In this case, the two PPO systems are aligned nearly parallel and rotating in phase - their upward and downward FAC regions overlap and enhance the associated modulations of the static main aurorae. The dawn UV power is largest roughly when the expected PPO upward FAC maxima pass and weakest during opposite PPO orientations, and varies by nearly a factor of 10. Consequently, the main oval seemingly disappears near dawn as the combined PPO downward FAC regions sweep over and negate the subcorotational system's upward currents (see Fig. 1b). While this modulation should theoretically be of comparable strength at all LTs (Hunt et al., 2016), it is here barely discernible at dusk. This difference in modulation amplitude agrees with statistical findings (Bader et al., 2018) and might be related to a seemingly larger spread of the PPO currents at dusk than at dawn (Andrews, Cowley, Dougherty, & Provan, 2010).

Neither the keogram (Fig. 1d) nor the summed dawn and dusk UV powers (Fig. 1e) show an asymmetry as expected during periods of significant solar wind driving - this is not surprising, as the time period considered here shows rather quiet auroral conditions, probably indicating quiet solar wind conditions and low Dungey cycle activity. Surprisingly though, the dusk side is noticeably brighter than the dawn side during most of the observation sequence. This can partly be explained with quasiperiodic flashes, possibly a sign of small-scale magnetodisc reconnection observed preferentially at dusk (Bader,

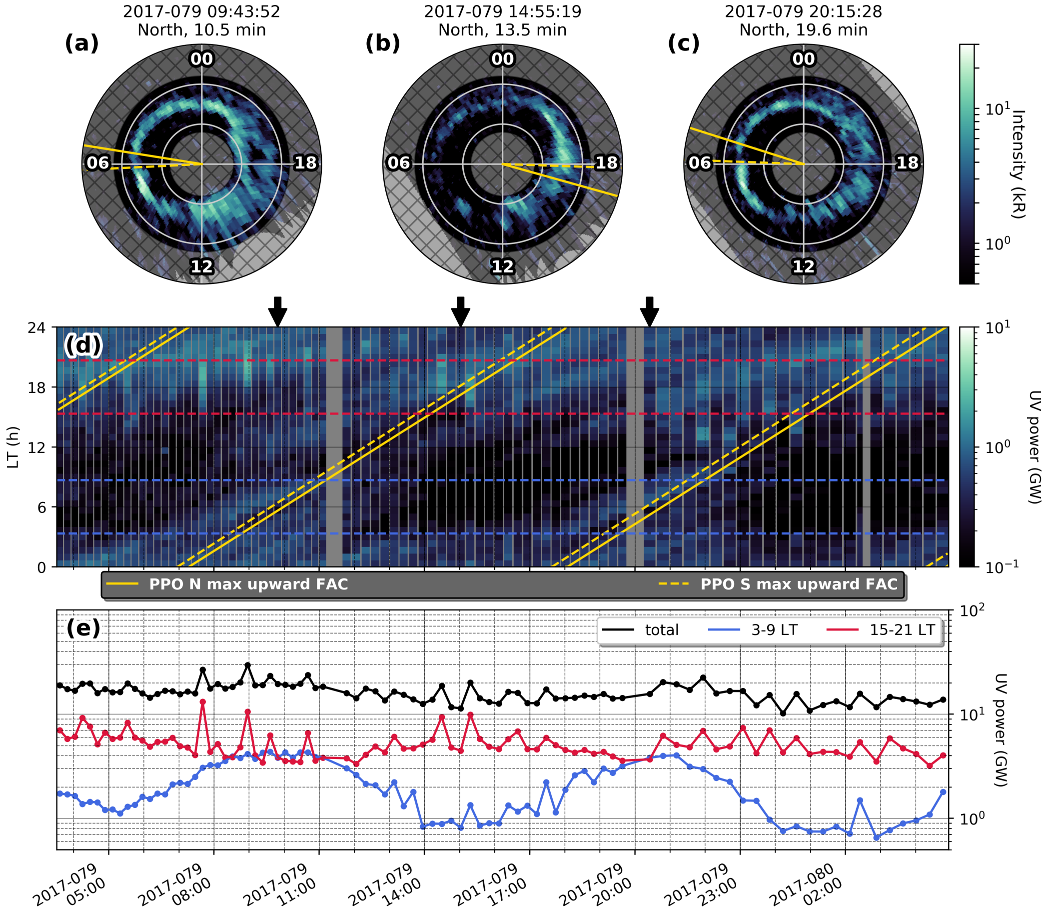

Figure 1. Ultraviolet (UV) auroral power keogram, quiet auroral conditions (2017 DOY 79-80). (a-c) Three UVIS images within this sequence, each about 5 − 6 h apart. The view is from above the planet down onto the north pole, with noon / the sun toward the bottom. White numbers around each image mark local time (LT), and grey concentric circles mark the northern colatitude in steps of 10°. The grey shaded and hatched regions (colatitudes > 22° and < 8°) were ignored for the integration of UV powers. The start and exposure time of each observation are given on top. Shown is the background-subtracted auroral brightness in kilo-Rayleigh; note the logarithmic scale. (d) UV power keogram of all images in this sequence; logarithmic power scale. The UV power between 8 − 22° colatitude was integrated in 36 LT bins for each image, and is arranged by the image collection time such that UT increases to the right. Diagonal lines mark planetary period oscillation (PPO) upward field-aligned current regions propagating around the planet at their respective PPO rotation rate. Dashed horizontal lines limit the “dawn” (blue) and “dusk” (red) LT bins whose UV powers were added for the line plots shown in the bottom panel. Black arrows on top of the panel mark the collection times of the example images shown in (a-c).(e) Line plots of the total, dawn and dusk UV powers.

Badman, Yao, et al., 2019). These have been shown to occur near-constantly and manifest as spikes in the dusk power (Fig. 1e), but they do not fully account for the underlying steady asymmetry between dawn and dusk which we observe here. At Jupiter, a similar asymmetry was observed and suggested to be related to a partial ring current in the nightside magnetosphere (Bonfond et al., 2015), but it is unclear whether a similar process could be important in Saturn's magnetosphere.

The case study presented in Fig. 1 is not the only quiet sequence observed. Considering only sequences with quasi-continuous coverage of at least one Saturn rotation, we find additional quiet sequences at 2014 DOY 130/147/158-159/311 (Supporting Fig. S2) - including overall 476 images with 67 h of total exposure time, corresponding to just over 6 Saturn rotations. A UV power-LT histogram for these images is shown in Figure 2a, with the mean and median power per LT added as line plots; the dawn and dusk slices of this histogram are compared in Figure 2b. We observe similar UV powers through all LTs, disagreeing with previously discussed UV and IR auroral intensity distributions (e.g., Bader et al., 2018; Badman et al., 2011; Carbary, 2012; Kinrade et al., 2018; Lamy et al., 2009, 2018; Nichols et al., 2016) with a brightness peak at dawn probably due to our choice of quiet periods. Centered on roughly 0.5 GW per 40 min LT bin, the powers are more variable and feature a more prominent tail toward lower powers at dawn/noon than at dusk/midnight. The occurrence of UV powers below the lower histogram limit (see Fig. 2b) is much larger at dawn, indicating longer intervals with a complete absence of auroral emissions.

There appears to be a dip in the average power at noon, somewhat reminiscent of the noon discontinuity in the Jovian main emission (e.g., Radioti et al., 2008; Ray, Achilleos, Vogt, & Yates, 2014). The currents associated with Jupiter's main emission are thought to be internally driven by the breakdown of corotation in the magnetodisc, which is less significant at the solar wind-compressed dayside (e.g., Chané, Saur, Keppens, & Poedts, 2017).

4 Typical auroral conditions and periodic magnetotail dynamics

Figure 2c-d shows a power histogram of all UVIS images between 2014 DOY 144-162. It includes 896 images, corresponding to ~ 122 h of exposure within the ~ 411 h observation window - a dataset quite representative of Saturn's typical auroral dynamics, likely capturing a variety of different solar wind conditions. As each observation block covers roughly one full Saturn rotation / PPO phase cycle or more, we assume no significant bias in PPO phases. A keogram of the entire set is shown in Supporting Fig. S3, including solar wind properties propagated from OMNI which indicate initially average solar wind conditions, likely with average Dungey cycle activity, followed by rather quiet conditions. Note that two of the observation blocks (2014 DOY 147/158-159) were considered quiet aurora and included in the corresponding analysis above as well as here.

Fig. 2c differs from the histogram of the quiet aurora (Fig. 2a) significantly only at dawn to post-noon LTs. We see a much wider spread in UV power at dawn than in quiet conditions, but do not observe a significant statistical dawn brightening (see Fig. 2d). On the contrary, again the median UV power is larger at dusk than at dawn. The mean and median UV power distributions (2c) are in close agreement between noon and midnight, but clearly differ near dawn - the mean maximizing here, while the median minimizes. The mean auroral power agrees very well with intensity averages of previous observations which all showed a distinct peak between 6-9 LT (e.g., Bader et al., 2018; Badman et al., 2011; Carbary, 2012; Kinrade et al., 2018; Lamy et al., 2009, 2018; Nichols et al., 2016) - but, as seen here, the mean UV intensity/power is obviously not a good representation of the typical state of the aurora. The median directly shows that in more cases than not, the dawn aurora is dimmer than the dusk aurora and not brighter; it is the few transient high-power events subcorotating through dawn which skew the mean

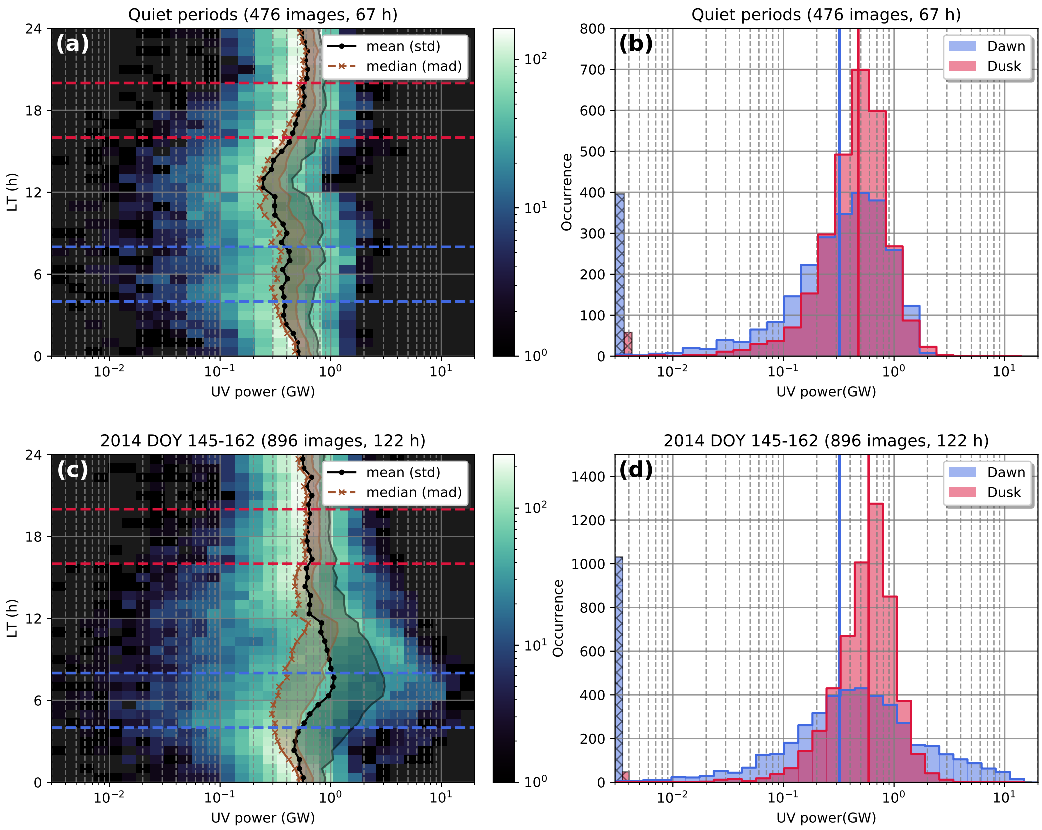

Figure 2. Ultraviolet (UV) auroral power histograms, quiet and average auroral conditions. (a) UV power histogram of 5 sequences with quiet auroral conditions (2014 DOY 130/147/158-159/311 and 2017 DOY 79-80, see Supporting Fig. S2), including 476 images with overall 67 hours of observations. Local time (LT) is on the vertical and (latitudinally integrated) UV power on the horizontal axis, the occurrence (number of observations) is shown in logarithmic color scale. Note the logarithmic UV power scaling on the horizontal axis. The mean (median) UV power per LT bin are shown in black (brown), with the standard deviation (median absolute deviation) indicated with a shaded area to the right of the graph. (b) Dawn (blue) and dusk (red) histograms, summed from all data enclosed by the blue/red-dashed lines in panel (a). Hatched bars to the left show the occurrence of bins with UV powers lower than the bottom limit of the graph. Solid vertical lines mark the median UV power per LT bin at dawn/dusk. (c-d) UV power histogram of 2014 DOY 144-162 (keograms in Fig. 4 and Supporting Figs. S3 and S4), including 896 images with an overall exposure time of 122 h. Same format as (a-b).

power to unrepresentative high values at these LTs. Figure 3 compares the mean and median brightness of the actual images in this dataset.

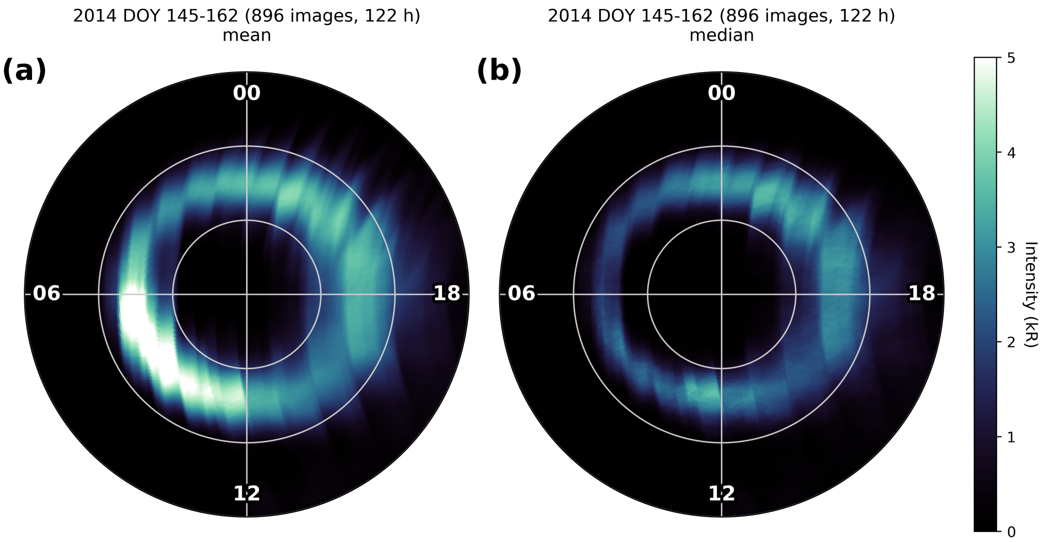

Figure 3. Comparison between Saturn's mean and median northern ultraviolet auroral brightness between 2014 DOY 145-162. The view is from above Saturn onto the planet's northern pole, with local noon to the bottom. Bold white numbers indicate local time; the northern colatitude from the pole is marked by grey concentric circles in 10° steps. The auroral brightness in kilo-Rayleigh is shown in color scale. (a) Mean and (b) median auroral brightness of all images.

A detailed view of the 2014 DOY 156-162 keograms is shown in Figure 4 (Supporting Fig. S4 shows 2014 DOY 144-149). The top row of panels shows an example UVIS image from each observation block - note that the observation geometry worsens toward the end, with the last images lacking coverage beyond $\sim 20^\circ$ colatitude from the pole between 18$-$24 LT. The integrated UV powers at these LTs are hence more uncertain as empty pixels have been filled with longitudinally averaged values of each latitudinal bin before integration.

The quiet auroral oval is overlaid with repeated powerful auroral plasma injection events (Mitchell et al., 2015) at Saturn's dawn side, which almost never rotate past noon as the perturbed source population's free energy is gradually deposited in Saturn's atmosphere, generating aurorae. The related rotating injected hot plasma populations seen in energetic neutral atom images do not stall at noon, but continue rotating near-rigidly with diminishing intensity back into the night side sector where they appear to be reenergized with every pass (Carbary & Mitchell, 2017; Mitchell et al., 2009). All injections commence near dawn, indicating nightside reconnection and the consequent magnetic dipolarization (Yao et al., 2017) as a likely cause (Radioti et al., 2016); considering the significant bendback of the magnetic field at dawn, this LT region maps well into Saturn's nightside. An auroral signature of this process may be the result of particle acceleration and precipitation during the dipolarization (Mitchell et al., 2015).

The injection events vary strongly in power, but show a regularity indicating a trigger mechanism internal to Saturn's magnetosphere. One known instigator of magnetotail reconnection is the PPO-induced modulation of the current sheet thickness (Bradley, Cowley, Bunce, et al., 2018; Cowley & Provan, 2017; Jackman et al., 2016), which is most pronounced when the two PPO systems rotate in antiphase. This is the case in Figure 4e;

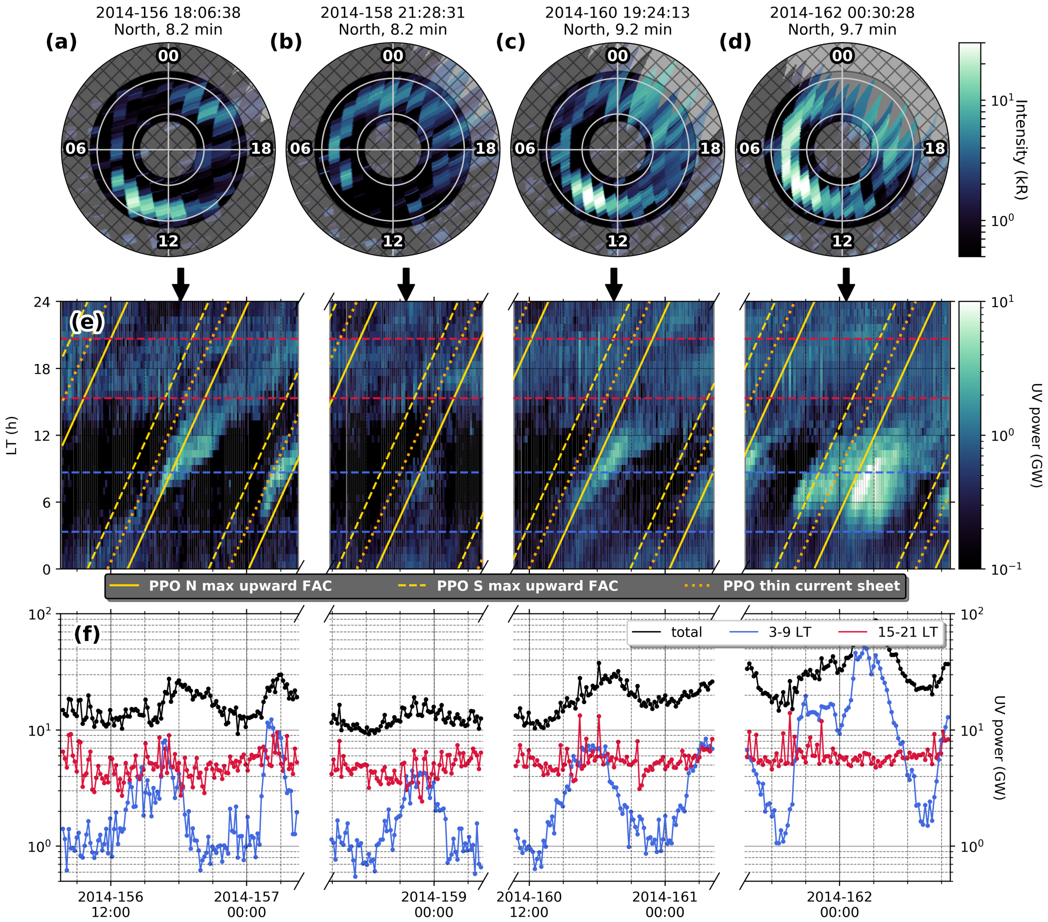

Figure 4. Ultraviolet auroral power keogram, typical auroral conditions (2014 DOY 156-162). Same format as Fig. 1, but showing four observation sequences with a broken time axis. In panel (e), orange dotted lines indicate where the planetary period oscillation-induced current sheet thinning is expected to be most pronounced, likely instigating reconnection.

the approximate location at which the current sheet is expected to be thinnest and reconnection is more likely to occur is indicated with orange-dotted lines. Most of the injections observed are triggered within some 3 h LT these highlighted locations, suggesting the PPO current sheet thinning effect to indeed be a main influence on the occurrence of the observed large-scale disturbances.

5 Discussion and conclusions

It is clear that Saturn's main aurorae are more dynamic than previous statistical studies may suggest. We conclude that the presently called "main aurorae" are associated with three different magnetospheric processes: the subcorotational FAC system, the two PPO FAC systems and the occurrence of large-scale magnetotail reconnection events.

The subcorotational system is a largely or completely LT-invariant system of FACs which are likely generated by flow shears between plasma populations subcorotating at different speeds in the middle and outer magnetosphere (Cowley, Bunce, & O'Rourke, 2004). This agrees with field-line mapping of the main aurorae which places the main upward FAC sheet at an equatorial distance beyond $10R_{\mathrm{S}}$, outwards from the middle ring current (e.g., Belenkaya et al., 2014; Bradley, Cowley, Provan, et al., 2018; Talboys et al., 2011). The flow of the solar wind and the associated Dungey cycle activity (e.g., Cowley, Bunce, & Prangé, 2004; Jackman & Cowley, 2006) seem to have little to no impact on this system, since no significant LT asymmetries in auroral FACs (Hunt et al., 2016) and auroral brightness are observed, contrary to previous findings (e.g., Bader et al., 2018; Badman et al., 2011; Carbary, 2012; Kinrade et al., 2018; Lamy et al., 2009, 2018; Nichols et al., 2016) where observed asymmetries were likely an artefact of small datasets and averaging procedures unsuitable for determining the full variability of Saturn's auroral dynamics. This is supported by earlier studies estimating the Dungey-cycle contribution to magnetic flux transport to be roughly an order of magnitude lower than the contribution arising from rotational flows in quiet solar wind conditions such that no asymmetry in auroral brightness is expected (e.g., Badman et al., 2005; Badman & Cowley, 2007). During solar wind compressions, significant asymmetries should theoretically arise (e.g., Badman & Cowley, 2007; Jackman et al., 2007) but will realistically be subsumed into the major auroral dynamics, i.e., poleward extending auroral storms, occurring simultaneously. The subcorotational system alone would cause a rather steady ring of upward FACs and associated auroral emissions around Saturn's poles corresponding to the region of highest flow shear, possibly with secondary emissions associated with corotation breakdown currents like Jupiter's main aurorae (Lamy et al., 2018; Stallard et al., 2008, 2007).

This subcorotational system is enhanced and reduced by the asymmetric PPO-related FACs flowing at the same latitudes (e.g., Bradley, Cowley, Provan, et al., 2018; Hunt et al., 2014, 2015). The slightly differing periods of the two PPO systems result in a double-sinusoidal modulation of the main oval's auroral brightness through LT, as the PPO and subcorotational FACs add up on one side of the planet but nearly negate each other on the opposite side (Bader et al., 2018) - we found this modulation to be significantly stronger at dawn than at dusk.

These two current systems combine to generate what should be considered the "main emission". Unintuitively though, the main (quasistatic and continuous) emission is often not dominant in Saturn's aurora, as it is quite dim (up to $\sim 10\,\mathrm{kR}$). It is overpowered significantly by large and bright patches, which are likely a consequence of magnetic dipolarization events (e.g., Jackman et al., 2013; Jia & Kivelson, 2012; Lamy et al., 2013; Radioti et al., 2016) and which usually emerge between midnight and dawn LTs. They subcorotate and usually disperse before reaching dusk. Their occurrence seems to be partly governed by the PPO-induced thinning of the current sheet (Bradley, Cowley, Bunce, et al., 2018; Cowley & Provan, 2017; Jackman et al., 2016); this was already observed in modelling studies (Jia & Kivelson, 2012; Zieger, Hansen, Gombosi, & De Zeeuw, 2010) and is likely related to similarly periodic plasma heating and ring current intensifications observed in energetic neutral atom measurements (Mitchell et al., 2009; Nichols et al., 2014). We observe such auroral plasma injection events about once per Saturn rotation, in rough agreement with direct plasmoid observations (Jackman et al., 2016; Jackman, Slavin, & Cowley, 2011) and Saturn's estimated magnetospheric refresh rate (Rymer et al., 2013).

Previous studies have further observed a clear dependence of magnetotail reconnection on solar wind conditions, as for example solar wind compression regions are known to trigger magnetotail reconnection and auroral storms (e.g., Badman et al., 2016; Clarke et al., 2005, 2009; Cowley et al., 2005; Crary et al., 2005; Kidder, Paty, Winglee, & Harnett, 2012; Palmaerts et al., 2018), roughly about once per week (Meredith, Cowley, & Nichols, 2014). Quiet solar wind conditions can lead to an expansion of the magnetotail and an accumulation of open flux as magnetotail reconnection is impeded (Badman et al., 2005; Badman, Jackman, Nichols, Clarke, & Gérard, 2014; Jackman et al., 2010), and fewer or no auroral injections are observed (Gérard et al., 2006). Moreover, higher magnetopause reconnection rates cause higher flux loading, thereby indirectly promoting magnetotail reconnection events (Badman et al., 2005, 2014; Jackman, 2004).

These results are an important step toward a better understanding of the global dynamics of Saturn's magnetosphere and the internal and external factors at play, providing a crucial framework for future studies. Analysing in-situ data from past Saturn missions as well as modelling the system theoretically in the light of these new findings will help investigate Saturn's global plasma circulation more thoroughly, helping unravel the physics of rotating magnetospheres in general.

Acknowledgments

All Cassini data are publicly available from the NASA Planetary Data System (`https://pds.jpl.nasa.gov`). PPO phase data (2004-2017) can be found on the University of Leicester Research Archive (`http://hdl.handle.net/2381/42436`). Cassini operations are supported by NASA (managed by the Jet Propulsion Laboratory) and European Space Agency (ESA). AB was funded by a Lancaster University FST studentship. SVB, LCR and JK were supported by STFC grant ST/R000816/1. SVB was also supported by an STFC Ernest Rutherford Fellowship ST/M005534/1. ZY acknowledges financial support from the Belgian Federal Science Policy Office (BELSPO) via the PRODEX Programme of ESA. TJB was supported by STFC Quota Studentship ST/N504117/1. GJH was supported by STFC consolidated grant ST/000692/2.

References

Andrews, D. J., Coates, A. J., Cowley, S. W. H., Dougherty, M. K., Lamy, L., Provan, G., & Zarka, P. (2010, December). Magnetospheric period oscillations at Saturn: Comparison of equatorial and high-latitude magnetic field periods with north and south Saturn kilometric radiation periods. *Journal of Geophysical Research: Space Physics*, *115*(A12252). Retrieved 2018-04-20, from `http://doi.wiley.com/10.1029/2010JA015666` doi: 10.1029/2010JA015666

Andrews, D. J., Cowley, S. W. H., Dougherty, M. K., & Provan, G. (2010, April). Magnetic field oscillations near the planetary period in Saturn's equatorial magnetosphere: Variation of amplitude and phase with radial distance and local time. *Journal of Geophysical Research: Space Physics*, *115*(A04212). Retrieved 2018-05-10, from `http://doi.wiley.com/10.1029/2009JA014729` doi: 10.1029/2009JA014729

Bader, A., Badman, S. V., Kinrade, J., Cowley, S. W. H., Provan, G., & Pryor, W.

(2019, February). Modulations of Saturn's UV auroral oval location by planetary period oscillations. *Journal of Geophysical Research: Space Physics*, *124*(2), 952–970. Retrieved 2019-03-23, from https://onlinelibrary.wiley.com/doi/abs/10.1029/2018JA026117 doi: 10.1029/2018JA026117

Bader, A., Badman, S. V., Kinrade, J., Cowley, S. W. H., Provan, G., & Pryor, W. R. (2018, October). Statistical planetary period oscillation signatures in Saturn's UV auroral intensity. *Journal of Geophysical Research: Space Physics*, *123*, 8459–8472. Retrieved 2018-10-30, from http://doi.wiley.com/10.1029/2018JA025855 doi: 10.1029/2018JA025855

Bader, A., Badman, S. V., Yao, Z. H., Kinrade, J., & Pryor, W. R. (2019, April). Observations of Continuous Quasiperiodic Auroral Pulsations on Saturn in High Time-Resolution UV Auroral Imagery. *Journal of Geophysical Research: Space Physics*, *124*, 2451–2465. Retrieved 2019-05-19, from https://onlinelibrary.wiley.com/doi/abs/10.1029/2018JA026320 doi: 10.1029/2018JA026320

Badman, S. V., Bunce, E. J., Clarke, J. T., Cowley, S. W. H., Gérard, J.-C., Grodent, D., & Milan, S. E. (2005). Open flux estimates in Saturn's magnetosphere during the January 2004 Cassini-HST campaign, and implications for reconnection rates. *Journal of Geophysical Research*, *110*(A11216). Retrieved 2018-04-20, from http://doi.wiley.com/10.1029/2005JA011240 doi: 10.1029/2005JA011240

Badman, S. V., & Cowley, S. W. H. (2007, May). Significance of Dungey-cycle flows in Jupiter's and Saturn's magnetospheres, and their identification on closed equatorial field lines. *Annales Geophysicae*, *25*(4), 941–951. Retrieved 2018-04-20, from http://www.ann-geophys.net/25/941/2007/ doi: 10.5194/angeo-25-941-2007

Badman, S. V., Jackman, C. M., Nichols, J. D., Clarke, J. T., & Gérard, J.-C. (2014, March). Open flux in Saturn's magnetosphere. *Icarus*, *231*, 137–145. Retrieved 2018-04-20, from http://linkinghub.elsevier.com/retrieve/pii/S0019103513005137 doi: 10.1016/j.icarus.2013.12.004

Badman, S. V., Masters, A., Hasegawa, H., Fujimoto, M., Radioti, A., Grodent, D., ... Coates, A. (2013, March). Bursty magnetic reconnection at Saturn's magnetopause. *Geophysical Research Letters*, *40*(6), 1027–1031. Retrieved 2018-04-20, from http://doi.wiley.com/10.1002/grl.50199 doi: 10.1002/grl.50199

Badman, S. V., Provan, G., Bunce, E. J., Mitchell, D. G., Melin, H., Cowley, S. W. H., ... Dougherty, M. K. (2016, January). Saturn's auroral morphology and field-aligned currents during a solar wind compression. *Icarus*, *263*, 83–93. Retrieved 2018-04-20, from http://linkinghub.elsevier.com/retrieve/pii/S0019103514006423 doi: 10.1016/j.icarus.2014.11.014

Badman, S. V., Tao, C., Grocott, A., Kasahara, S., Melin, H., Brown, R. H., ... Stallard, T. (2011, December). Cassini VIMS observations of latitudinal and hemispheric variations in Saturn's infrared auroral intensity. *Icarus*, *216*(2), 367–375. Retrieved 2019-01-18, from https://linkinghub.elsevier.com/retrieve/pii/S0019103511003836 doi: 10.1016/j.icarus.2011.09.031

Belenkaya, E. S., Cowley, S. W. H., Meredith, C. J., Nichols, J. D., Kalegaev, V. V., Alexeev, I. I., ... Blokhina, M. S. (2014, June). Magnetospheric magnetic field modelling for the 2011 and 2012 HST Saturn aurora campaigns - implications for auroral source regions. *Annales Geophysicae*, *32*(6), 689–704. Retrieved 2018-04-23, from http://www.ann-geophys.net/32/689/2014/ doi: 10.5194/angeo-32-689-2014

Bonfond, B., Gustin, J., Gérard, J.-C., Grodent, D., Radioti, A., Palmaerts, B., ... Tao, C. (2015, October). The far-ultraviolet main auroral emission at Jupiter - Part 1: Dawn-dusk brightness asymmetries. *Annales Geophysicae*, *33*(10), 1203–1209. Retrieved 2019-03-18, from https://www.ann-geophys.net/33/

1203/2015/ doi: 10.5194/angeo-33-1203-2015
Bradley, T. J., Cowley, S. W. H., Bunce, E. J., Smith, A. W., Jackman, C. M., & Provan, G. (2018, November). Planetary Period Modulation of Reconnection Bursts in Saturn's Magnetotail. *Journal of Geophysical Research: Space Physics*, *123*(11), 9476–9507. Retrieved 2019-05-16, from https://onlinelibrary.wiley.com/doi/abs/10.1029/2018JA025932 doi: 10.1029/2018JA025932
Bradley, T. J., Cowley, S. W. H., Provan, G., Hunt, G. J., Bunce, E. J., Wharton, S. J., ... Dougherty, M. K. (2018, May). Field-aligned currents in Saturn's nightside magnetosphere: Subcorotation and planetary period oscillation components during northern spring. *Journal of Geophysical Research: Space Physics*, *123*, 3602–3636. Retrieved 2018-05-23, from http://doi.wiley.com/10.1029/2017JA024885 doi: 10.1029/2017JA024885
Brain, D. A., Halekas, J. S., Peticolas, L. M., Lin, R. P., Luhmann, J. G., Mitchell, D. L., ... Rème, H. (2006, January). On the origin of aurorae on Mars. *Geophysical Research Letters*, *33*(L01201). Retrieved 2019-01-27, from http://doi.wiley.com/10.1029/2005GL024782 doi: 10.1029/2005GL024782
Carbary, J. F. (2012, June). The morphology of Saturn's ultraviolet aurora. *Journal of Geophysical Research: Space Physics*, *117*(A06210). Retrieved 2018-04-20, from http://doi.wiley.com/10.1029/2012JA017670 doi: 10.1029/2012JA017670
Carbary, J. F., & Mitchell, D. G. (2017, July). Midnight flash model of energetic neutral atom periodicities at Saturn: Midnight Flash Model. *Journal of Geophysical Research: Space Physics*, *122*(7), 7110–7117. Retrieved 2018-11-20, from http://doi.wiley.com/10.1002/2017JA024296 doi: 10.1002/2017JA024296
Chané, E., Saur, J., Keppens, R., & Poedts, S. (2017). How is the Jovian main auroral emission affected by the solar wind? *Journal of Geophysical Research: Space Physics*, *122*, 1960–1978. Retrieved 2019-02-25, from http://doi.wiley.com/10.1002/2016JA023318 doi: 10.1002/2016JA023318
Clarke, J. T., Connerney, J., Crary, F., Dougherty, M., Kurth, W., Cowley, S. W. H., ... Kim, J. (2005). Morphological differences between Saturn's ultraviolet aurorae and those of Earth and Jupiter. *Nature*, *433*, 3.
Clarke, J. T., Nichols, J., Gérard, J.-C., Grodent, D., Hansen, K. C., Kurth, W., ... Cecconi, B. (2009, May). Response of Jupiter's and Saturn's auroral activity to the solar wind. *Journal of Geophysical Research: Space Physics*, *114*(A05210). Retrieved 2018-04-20, from http://doi.wiley.com/10.1029/2008JA013694 doi: 10.1029/2008JA013694
Cowley, S. W. H., Badman, S. V., Bunce, E. J., Clarke, J. T., Gérard, J.-C., Grodent, D. C., ... Yeoman, T. K. (2005). Reconnection in a rotation-dominated magnetosphere and its relation to Saturn's auroral dynamics. *Journal of Geophysical Research*, *110*(A02201). Retrieved 2018-04-20, from http://doi.wiley.com/10.1029/2004JA010796 doi: 10.1029/2004JA010796
Cowley, S. W. H., & Bunce, E. J. (2001, August). Origin of the main auroral oval in Jupiter's coupled magnetosphere–ionosphere system. *Planetary and Space Science*, *49*(10-11), 1067–1088. Retrieved 2019-01-18, from http://linkinghub.elsevier.com/retrieve/pii/S0032063300001677 doi: 10.1016/S0032-0633(00)00167-7
Cowley, S. W. H., & Bunce, E. J. (2003). Corotation-driven magnetosphere-ionosphere coupling currents in Saturn's magnetosphere and their relation to the auroras. *Annales Geophysicae*, *21*(8), 1691–1707. Retrieved 2018-04-20, from http://www.ann-geophys.net/21/1691/2003/ doi: 10.5194/angeo-21-1691-2003
Cowley, S. W. H., Bunce, E. J., & O'Rourke, J. M. (2004, May). A simple quantitative model of plasma flows and currents in Saturn's polar ionosphere. *Journal*

of Geophysical Research, *109*(A05212). Retrieved 2018-04-20, from http://doi.wiley.com/10.1029/2003JA010375 doi: 10.1029/2003JA010375
Cowley, S. W. H., Bunce, E. J., & Prangé, R. (2004, April). Saturn's polar ionospheric flows and their relation to the main auroral oval. *Annales Geophysicae*, *22*(4), 1379–1394. Retrieved 2018-04-23, from http://www.ann-geophys.net/22/1379/2004/ doi: 10.5194/angeo-22-1379-2004
Cowley, S. W. H., & Provan, G. (2017, June). Planetary period modulations of Saturn's magnetotail current sheet during northern spring: Observations and modeling. *Journal of Geophysical Research: Space Physics*, *122*(6), 6049–6077. Retrieved 2018-08-08, from http://doi.wiley.com/10.1002/2017JA023993 doi: 10.1002/2017JA023993
Crary, F. J., Clarke, J. T., Dougherty, M. K., Hanlon, P. G., Hansen, K. C., Steinberg, J. T., … Young, D. T. (2005, February). Solar wind dynamic pressure and electric field as the main factors controlling Saturn's aurorae. *Nature*, *433*, 720. Retrieved from https://doi.org/10.1038/nature03333 doi: 10.1038/nature03333
Delamere, P. A., & Bagenal, F. (2010, October). Solar wind interaction with Jupiter's magnetosphere. *Journal of Geophysical Research: Space Physics*, *115*(A10201). Retrieved 2018-10-10, from http://doi.wiley.com/10.1029/2010JA015347 doi: 10.1029/2010JA015347
Delamere, P. A., Wilson, R. J., Eriksson, S., & Bagenal, F. (2013, January). Magnetic signatures of Kelvin-Helmholtz vortices on Saturn's magnetopause: Global survey. *Journal of Geophysical Research: Space Physics*, *118*(1), 393–404. Retrieved 2018-10-16, from http://doi.wiley.com/10.1029/2012JA018197 doi: 10.1029/2012JA018197
Desroche, M., Bagenal, F., Delamere, P. A., & Erkaev, N. (2013, June). Conditions at the magnetopause of Saturn and implications for the solar wind interaction. *Journal of Geophysical Research: Space Physics*, *118*(6), 3087–3095. Retrieved 2019-07-10, from http://doi.wiley.com/10.1002/jgra.50294 doi: 10.1002/jgra.50294
Dungey, J. W. (1961, January). Interplanetary magnetic field and the auroral zones. *Physical Review Letters*, *6*(2), 47–48. Retrieved 2019-03-06, from https://link.aps.org/doi/10.1103/PhysRevLett.6.47 doi: 10.1103/PhysRevLett.6.47
Esposito, L. W., Barth, C. A., Colwell, J. E., Lawrence, G. M., McClintock, W. E., Stewart, A. I. F., … Yung, Y. L. (2004, November). The Cassini Ultraviolet Imaging Spectrograph investigation. *Space Science Reviews*, *115*(1-4), 299–361. Retrieved 2018-06-16, from https://link.springer.com/article/10.1007/s11214-004-1455-8 doi: 10.1007/s11214-004-1455-8
Gustin, J., Grodent, D., Radioti, A., Pryor, W., Lamy, L., & Ajello, J. (2017, March). Statistical study of Saturn's auroral electron properties with Cassini/UVIS FUV spectral images. *Icarus*, *284*, 264–283. Retrieved 2018-04-20, from http://linkinghub.elsevier.com/retrieve/pii/S0019103516304705 doi: 10.1016/j.icarus.2016.11.017
Gustin, J., Grodent, D., Ray, L., Bonfond, B., Bunce, E., Nichols, J., & Ozak, N. (2016, April). Characteristics of north jovian aurora from STIS FUV spectral images. *Icarus*, *268*, 215–241. Retrieved 2018-04-20, from http://linkinghub.elsevier.com/retrieve/pii/S0019103515006144 doi: 10.1016/j.icarus.2015.12.048
Gérard, J.-C., Bonfond, B., Gustin, J., Grodent, D., Clarke, J. T., Bisikalo, D., & Shematovich, V. (2009, January). Altitude of Saturn's aurora and its implications for the characteristic energy of precipitated electrons. *Geophysical Research Letters*, *36*(L02202). Retrieved 2018-04-24, from http://doi.wiley.com/10.1029/2008GL036554 doi: 10.1029/2008GL036554
Gérard, J.-C., Grodent, D., Cowley, S. W. H., Mitchell, D. G., Kurth, W. S., Clarke,

J. T., ... Coates, A. J. (2006, December). Saturn's auroral morphology and activity during quiet magnetospheric conditions. *Journal of Geophysical Research*, *111*(A12210). Retrieved 2019-01-25, from `http://doi.wiley.com/10.1029/2006JA011965` doi: 10.1029/2006JA011965

Hill, T. W. (2001, May). The Jovian auroral oval. *Journal of Geophysical Research: Space Physics*, *106*(A5), 8101–8107. Retrieved 2019-01-25, from `http://doi.wiley.com/10.1029/2000JA000302` doi: 10.1029/2000JA000302

Hunt, G. J., Cowley, S. W. H., Provan, G., Bunce, E. J., Alexeev, I. I., Belenkaya, E. S., ... Coates, A. J. (2014, December). Field-aligned currents in Saturn's southern nightside magnetosphere: Subcorotation and planetary period oscillation components. *Journal of Geophysical Research: Space Physics*, *119*(12), 9847–9899. Retrieved 2018-04-20, from `http://doi.wiley.com/10.1002/2014JA020506` doi: 10.1002/2014JA020506

Hunt, G. J., Cowley, S. W. H., Provan, G., Bunce, E. J., Alexeev, I. I., Belenkaya, E. S., ... Coates, A. J. (2015, September). Field-aligned currents in Saturn's northern nightside magnetosphere: Evidence for interhemispheric current flow associated with planetary period oscillations. *Journal of Geophysical Research: Space Physics*, *120*(9), 7552–7584. Retrieved 2018-04-20, from `http://doi.wiley.com/10.1002/2015JA021454` doi: 10.1002/2015JA021454

Hunt, G. J., Cowley, S. W. H., Provan, G., Bunce, E. J., Alexeev, I. I., Belenkaya, E. S., ... Coates, A. J. (2016, August). Field-aligned currents in Saturn's magnetosphere: Local time dependence of southern summer currents in the dawn sector between midnight and noon. *Journal of Geophysical Research: Space Physics*, *121*(8), 7785–7804. Retrieved 2018-04-20, from `http://doi.wiley.com/10.1002/2016JA022712` doi: 10.1002/2016JA022712

Isbell, J., Dessler, A. J., & Waite, J. H. (1984). Magnetospheric energization by interaction between planetary spin and the solar wind. *Journal of Geophysical Research*, *89*(A12), 10716. Retrieved 2019-03-14, from `http://doi.wiley.com/10.1029/JA089iA12p10716` doi: 10.1029/JA089iA12p10716

Jackman, C. M. (2004). Interplanetary magnetic field at ~9 AU during the declining phase of the solar cycle and its implications for Saturn's magnetospheric dynamics. *Journal of Geophysical Research*, *109*(A11203). Retrieved 2019-03-11, from `http://doi.wiley.com/10.1029/2004JA010614` doi: 10.1029/2004JA010614

Jackman, C. M., Achilleos, N., Cowley, S. W., Bunce, E. J., Radioti, A., Grodent, D., ... Pryor, W. (2013, July). Auroral counterpart of magnetic field dipolarizations in Saturn's tail. *Planetary and Space Science*, *82-83*, 34–42. Retrieved 2018-04-20, from `http://linkinghub.elsevier.com/retrieve/pii/S003206331300069X` doi: 10.1016/j.pss.2013.03.010

Jackman, C. M., Arridge, C. S., Slavin, J. A., Milan, S. E., Lamy, L., Dougherty, M. K., & Coates, A. J. (2010, October). In situ observations of the effect of a solar wind compression on Saturn's magnetotail. *Journal of Geophysical Research: Space Physics*, *115*(A10240). Retrieved 2019-03-11, from `http://doi.wiley.com/10.1029/2010JA015312` doi: 10.1029/2010JA015312

Jackman, C. M., & Cowley, S. W. H. (2006, May). A model of the plasma flow and current in Saturn's polar ionosphere under conditions of strong Dungey cycle driving. *Annales Geophysicae*, *24*(3), 1029–1055. Retrieved 2019-01-08, from `http://www.ann-geophys.net/24/1029/2006/` doi: 10.5194/angeo-24-1029-2006

Jackman, C. M., Provan, G., & Cowley, S. W. H. (2016, April). Reconnection events in Saturn's magnetotail: Dependence of plasmoid occurrence on planetary period oscillation phase. *Journal of Geophysical Research: Space Physics*, *121*(4), 2922–2934. Retrieved 2018-08-08, from `http://doi.wiley.com/10.1002/2015JA021985` doi: 10.1002/2015JA021985

Jackman, C. M., Russell, C. T., Southwood, D. J., Arridge, C. S., Achilleos, N., & Dougherty, M. K. (2007, June). Strong rapid dipolarizations in Saturn's magnetotail: In situ evidence of reconnection. *Geophysical Research Letters*, *34*(11). Retrieved 2018-04-20, from http://doi.wiley.com/10.1029/2007GL029764 doi: 10.1029/2007GL029764

Jackman, C. M., Slavin, J. A., & Cowley, S. W. H. (2011, October). Cassini observations of plasmoid structure and dynamics: Implications for the role of magnetic reconnection in magnetospheric circulation at Saturn. *Journal of Geophysical Research: Space Physics*, *116*(A10212). Retrieved 2018-04-20, from http://doi.wiley.com/10.1029/2011JA016682 doi: 10.1029/2011JA016682

Jia, X., & Kivelson, M. G. (2012, November). Driving Saturn's magnetospheric periodicities from the upper atmosphere/ionosphere: Magnetotail response to dual sources. *Journal of Geophysical Research: Space Physics*, *117*(A11219). Retrieved 2018-05-28, from http://doi.wiley.com/10.1029/2012JA018183 doi: 10.1029/2012JA018183

Jia, X., Kivelson, M. G., & Gombosi, T. I. (2012, April). Driving Saturn's magnetospheric periodicities from the upper atmosphere/ionosphere. *Journal of Geophysical Research: Space Physics*, *117*(A04215). Retrieved 2018-04-20, from http://doi.wiley.com/10.1029/2011JA017367 doi: 10.1029/2011JA017367

Kidder, A., Paty, C. S., Winglee, R. M., & Harnett, E. M. (2012, July). External triggering of plasmoid development at Saturn. *Journal of Geophysical Research: Space Physics*, *117*(A07206). Retrieved 2019-02-07, from http://doi.wiley.com/10.1029/2012JA017625 doi: 10.1029/2012JA017625

Kinrade, J., Badman, S. V., Provan, G., Cowley, S. W. H., Lamy, L., & Bader, A. (2018, August). Saturn's Northern Auroras and Their Modulation by Rotating Current Systems During Late Northern Spring in Early 2014. *Journal of Geophysical Research: Space Physics*, *123*(8), 6289–6306. Retrieved 2018-11-01, from http://doi.wiley.com/10.1029/2018JA025426 doi: 10.1029/2018JA025426

Lamy, L., Cecconi, B., Prangé, R., Zarka, P., Nichols, J. D., & Clarke, J. T. (2009, October). An auroral oval at the footprint of Saturn's kilometric radio sources, colocated with the UV aurorae. *Journal of Geophysical Research: Space Physics*, *114*(A10212). Retrieved 2018-11-14, from http://doi.wiley.com/10.1029/2009JA014401 doi: 10.1029/2009JA014401

Lamy, L., Prangé, R., Pryor, W., Gustin, J., Badman, S. V., Melin, H., … Brandt, P. C. (2013, August). Multispectral simultaneous diagnosis of Saturn's aurorae throughout a planetary rotation. *Journal of Geophysical Research: Space Physics*, *118*(8), 4817–4843. Retrieved 2018-04-20, from http://doi.wiley.com/10.1002/jgra.50404 doi: 10.1002/jgra.50404

Lamy, L., Prangé, R., Tao, C., Kim, T., Badman, S. V., Zarka, P., … Radioti, A. (2018, September). Saturn's Northern Aurorae at Solstice From HST Observations Coordinated With Cassini's Grand Finale. *Geophysical Research Letters*, *45*(18), 9353–9362. Retrieved 2019-05-16, from http://doi.wiley.com/10.1029/2018GL078211 doi: 10.1029/2018GL078211

Masters, A., Eastwood, J. P., Swisdak, M., Thomsen, M. F., Russell, C. T., Sergis, N., … Krimigis, S. M. (2012, April). The importance of plasma β conditions for magnetic reconnection at Saturn's magnetopause. *Geophysical Research Letters*, *39*(L08103). Retrieved 2019-07-10, from http://doi.wiley.com/10.1029/2012GL051372 doi: 10.1029/2012GL051372

Masters, A., Fujimoto, M., Hasegawa, H., Russell, C. T., Coates, A. J., & Dougherty, M. K. (2014, March). Can magnetopause reconnection drive Saturn's magnetosphere?: Saturn reconnection driving. *Geophysical Research Letters*, *41*(6), 1862–1868. Retrieved 2019-07-10, from http://doi.wiley.com/

10.1002/2014GL059288 doi: 10.1002/2014GL059288

Meredith, C. J., Alexeev, I. I., Badman, S. V., Belenkaya, E. S., Cowley, S. W. H., Dougherty, M. K., ... Nichols, J. D. (2014, March). Saturn's dayside ultraviolet auroras: Evidence for morphological dependence on the direction of the upstream interplanetary magnetic field. *Journal of Geophysical Research: Space Physics*, *119*(3), 1994–2008. Retrieved 2018-04-20, from http://doi.wiley.com/10.1002/2013JA019598 doi: 10.1002/2013JA019598

Meredith, C. J., Cowley, S. W. H., & Nichols, J. D. (2014, December). Survey of Saturn auroral storms observed by the Hubble Space Telescope: Implications for storm time scales: Saturn's auroral storms. *Journal of Geophysical Research: Space Physics*, *119*(12), 9624–9642. Retrieved 2018-08-06, from http://doi.wiley.com/10.1002/2014JA020601 doi: 10.1002/2014JA020601

Milan, S. E., Bunce, E. J., Cowley, S. W. H., & Jackman, C. M. (2005). Implications of rapid planetary rotation for the Dungey magnetotail of Saturn. *Journal of Geophysical Research*, *110*(A03209). Retrieved 2019-07-10, from http://doi.wiley.com/10.1029/2004JA010716 doi: 10.1029/2004JA010716

Milan, S. E., Lester, M., Cowley, S. W. H., Oksavik, K., Brittnacher, M., Greenwald, R. A., ... Villain, J.-P. (2003). Variations in the polar cap area during two substorm cycles. *Annales Geophysicae*, *21*(5), 1121–1140. Retrieved 2019-02-07, from http://www.ann-geophys.net/21/1121/2003/ doi: 10.5194/angeo-21-1121-2003

Mitchell, D. G., Brandt, P. C., Carbary, J. F., Kurth, W. S., Krimigis, S. M., Paranicas, C., ... Pryor, W. R. (2015, January). Injection, Interchange, and Reconnection: Energetic Particle Observations in Saturn's Magnetosphere. In A. Keiling, C. M. Jackman, & P. A. Delamere (Eds.), *Magnetotails in the Solar System* (pp. 327–343). Hoboken, NJ: John Wiley & Sons, Inc. Retrieved 2018-09-26, from http://doi.wiley.com/10.1002/9781118842324.ch19 doi: 10.1002/9781118842324.ch19

Mitchell, D. G., Krimigis, S. M., Paranicas, C., Brandt, P. C., Carbary, J. F., Roelof, E. C., ... Pryor, W. R. (2009, December). Recurrent energization of plasma in the midnight-to-dawn quadrant of Saturn's magnetosphere, and its relationship to auroral UV and radio emissions. *Planetary and Space Science*, *57*(14-15), 1732–1742. Retrieved 2018-04-20, from http://linkinghub.elsevier.com/retrieve/pii/S0032063309001044 doi: 10.1016/j.pss.2009.04.002

Nichols, J. D., Badman, S. V., Bunce, E. J., Clarke, J. T., Cowley, S. W. H., Hunt, G. J., & Provan, G. (2016, January). Saturn's northern auroras as observed using the Hubble Space Telescope. *Icarus*, *263*, 17–31. Retrieved 2018-04-20, from http://linkinghub.elsevier.com/retrieve/pii/S001910351500411X doi: 10.1016/j.icarus.2015.09.008

Nichols, J. D., V.Badman, S., Baines, K. H., Brown, R. H., Bunce, E. J., Clarke, J. T., ... Stallard, T. S. (2014, May). Dynamic auroral storms on Saturn as observed by the Hubble Space Telescope. *Geophysical Research Letters*, *41*(10), 3323–3330. Retrieved 2018-04-20, from http://doi.wiley.com/10.1002/2014GL060186 doi: 10.1002/2014GL060186

Palmaerts, B., Radioti, A., Grodent, D., Yao, Z. H., Bradley, T. J., Roussos, E., ... Pryor, W. R. (2018, July). Auroral storm and polar arcs at Saturn — Final Cassini/UVIS auroral observations. *Geophysical Research Letters*, *45*(14), 6832–6842. Retrieved 2019-01-25, from http://doi.wiley.com/10.1029/2018GL078094 doi: 10.1029/2018GL078094

Provan, G., Andrews, D. J., Cecconi, B., Cowley, S. W. H., Dougherty, M. K., Lamy, L., & Zarka, P. M. (2011, April). Magnetospheric period magnetic field oscillations at Saturn: Equatorial phase "jitter" produced by superposition of southern and northern period oscillations. *Journal of Geophysical Research: Space*

Physics, *116* (A04225). Retrieved 2018-04-27, from http://doi.wiley.com/10.1029/2010JA016213 doi: 10.1029/2010JA016213

Provan, G., Cowley, S. W. H., Bradley, T. J., Bunce, E. J., Hunt, G. J., & Dougherty, M. K. (2018, May). Planetary period oscillations in Saturn's magnetosphere: Cassini magnetic field observations over the northern summer solstice interval. *Journal of Geophysical Research: Space Physics*, *123*, 3859–3899. Retrieved 2018-06-06, from http://doi.wiley.com/10.1029/2018JA025237 doi: 10.1029/2018JA025237

Provan, G., Cowley, S. W. H., Lamy, L., Bunce, E. J., Hunt, G. J., Zarka, P., & Dougherty, M. K. (2016, October). Planetary period oscillations in Saturn's magnetosphere: Coalescence and reversal of northern and southern periods in late northern spring. *Journal of Geophysical Research: Space Physics*, *121* (10), 9829–9862. Retrieved 2018-04-20, from http://doi.wiley.com/10.1002/2016JA023056 doi: 10.1002/2016JA023056

Provan, G., Cowley, S. W. H., Sandhu, J., Andrews, D. J., & Dougherty, M. K. (2013, June). Planetary period magnetic field oscillations in Saturn's magnetosphere: Postequinox abrupt nonmonotonic transitions to northern system dominance. *Journal of Geophysical Research: Space Physics*, *118* (6), 3243–3264. Retrieved 2018-04-27, from http://doi.wiley.com/10.1002/jgra.50186 doi: 10.1002/jgra.50186

Radioti, A., Grodent, D., Gérard, J.-C., Bonfond, B., Gustin, J., Pryor, W., … Arridge, C. S. (2013, September). Auroral signatures of multiple magnetopause reconnection at Saturn. *Geophysical Research Letters*, *40* (17), 4498–4502. Retrieved 2018-04-20, from http://doi.wiley.com/10.1002/grl.50889 doi: 10.1002/grl.50889

Radioti, A., Grodent, D., Gérard, J.-C., Milan, S. E., Bonfond, B., Gustin, J., & Pryor, W. (2011, November). Bifurcations of the main auroral ring at Saturn: ionospheric signatures of consecutive reconnection events at the magnetopause. *Journal of Geophysical Research: Space Physics*, *116* (A11209). Retrieved 2018-04-20, from http://doi.wiley.com/10.1029/2011JA016661 doi: 10.1029/2011JA016661

Radioti, A., Grodent, D., Jia, X., Gérard, J.-C., Bonfond, B., Pryor, W., … Jackman, C. (2016, January). A multi-scale magnetotail reconnection event at Saturn and associated flows: Cassini/UVIS observations. *Icarus*, *263*, 75–82. Retrieved 2018-04-20, from http://linkinghub.elsevier.com/retrieve/pii/S0019103514006964 doi: 10.1016/j.icarus.2014.12.016

Radioti, A., Gérard, J.-C., Grodent, D., Bonfond, B., Krupp, N., & Woch, J. (2008, January). Discontinuity in Jupiter's main auroral oval. *Journal of Geophysical Research: Space Physics*, *113* (A01215). Retrieved 2019-01-18, from http://doi.wiley.com/10.1029/2007JA012610 doi: 10.1029/2007JA012610

Ray, L. C., Achilleos, N. A., Vogt, M. F., & Yates, J. N. (2014, June). Local time variations in Jupiter's magnetosphere-ionosphere coupling system. *Journal of Geophysical Research: Space Physics*, *119* (6), 4740–4751. Retrieved 2019-01-18, from http://doi.wiley.com/10.1002/2014JA019941 doi: 10.1002/2014JA019941

Rymer, A. M., Mitchell, D. G., Hill, T. W., Kronberg, E. A., Krupp, N., & Jackman, C. M. (2013, June). Saturn's magnetospheric refresh rate. *Geophysical Research Letters*, *40* (11), 2479–2483. Retrieved 2019-02-06, from http://doi.wiley.com/10.1002/grl.50530 doi: 10.1002/grl.50530

Sandel, B. R., & Broadfoot, A. L. (1981, August). Morphology of Saturn's aurora. *Nature*, *292* (5825), 679–682. Retrieved 2019-05-15, from http://www.nature.com/articles/292679a0 doi: 10.1038/292679a0

Sandel, B. R., Shemansky, D. E., Broadfoot, A. L., Holberg, J. B., Smith, G. R., Mcconnell, J. C., … Linick, S. (1982, January). Extreme Ultraviolet Observations from the Voyager 2 Encounter with Saturn. *Science*, *215* (4532), 548–553.

Retrieved 2018-11-14, from http://www.sciencemag.org/cgi/doi/10.1126/science.215.4532.548 doi: 10.1126/science.215.4532.548

Southwood, D. J., & Cowley, S. W. H. (2014, March). The origin of Saturn's magnetic periodicities: Northern and southern current systems. *Journal of Geophysical Research: Space Physics*, *119*(3), 1563–1571. Retrieved 2018-04-20, from http://doi.wiley.com/10.1002/2013JA019632 doi: 10.1002/2013JA019632

Southwood, D. J., & Kivelson, M. G. (2001, April). A new perspective concerning the influence of the solar wind on the Jovian magnetosphere. *Journal of Geophysical Research: Space Physics*, *106*(A4), 6123–6130. Retrieved 2019-01-25, from http://doi.wiley.com/10.1029/2000JA000236 doi: 10.1029/2000JA000236

Southwood, D. J., & Kivelson, M. G. (2007, December). Saturnian magnetospheric dynamics: Elucidation of a camshaft model. *Journal of Geophysical Research: Space Physics*, *112*(A12222). Retrieved 2019-01-24, from http://doi.wiley.com/10.1029/2007JA012254 doi: 10.1029/2007JA012254

Stallard, T., Miller, S., Melin, H., Lystrup, M., Cowley, S. W. H., Bunce, E. J., ... Dougherty, M. (2008, June). Jovian-like aurorae on Saturn. *Nature*, *453*(7198), 1083–1085. Retrieved 2018-04-20, from http://www.nature.com/articles/nature07077 doi: 10.1038/nature07077

Stallard, T., Smith, C., Miller, S., Melin, H., Lystrup, M., Aylward, A., ... Dougherty, M. (2007, November). Saturn's auroral/polar H+3 infrared emission: II. A comparison with plasma flow models. *Icarus*, *191*(2), 678–690. Retrieved 2018-04-23, from http://linkinghub.elsevier.com/retrieve/pii/S0019103507002606 doi: 10.1016/j.icarus.2007.05.016

Talboys, D. L., Bunce, E. J., Cowley, S. W. H., Arridge, C. S., Coates, A. J., & Dougherty, M. K. (2011, April). Statistical characteristics of field-aligned currents in Saturn's nightside magnetosphere. *Journal of Geophysical Research: Space Physics*, *116*(A04213). Retrieved 2018-05-11, from http://doi.wiley.com/10.1029/2010JA016102 doi: 10.1029/2010JA016102

Vasyliūnas, V. M. (1983). Plasma distribution and flow. In A. J. Dessler (Ed.), *Physics of the Jovian Magnetosphere* (pp. 395–453). Cambridge, UK: Cambridge University Press.

Vasyliūnas, V. M. (2016, February). Physical origin of pickup currents. *Annales Geophysicae*, *34*(1), 153–156. Retrieved 2019-06-15, from https://www.ann-geophys.net/34/153/2016/ doi: 10.5194/angeo-34-153-2016

Walach, M.-T., Milan, S. E., Murphy, K. R., Carter, J. A., Hubert, B. A., & Grocott, A. (2017, June). Comparative study of large-scale auroral signatures of substorms, steady magnetospheric convection events, and sawtooth events. *Journal of Geophysical Research: Space Physics*, *122*(6), 6357–6373. Retrieved 2019-07-12, from http://doi.wiley.com/10.1002/2017JA023991 doi: 10.1002/2017JA023991

Yao, Z. H., Grodent, D., Ray, L. C., Rae, I. J., Coates, A. J., Pu, Z. Y., ... Dunn, W. R. (2017, April). Two fundamentally different drivers of dipolarizations at Saturn. *Journal of Geophysical Research: Space Physics*, *122*(4), 4348–4356. Retrieved 2018-04-20, from http://doi.wiley.com/10.1002/2017JA024060 doi: 10.1002/2017JA024060

Zieger, B., Hansen, K. C., Gombosi, T. I., & De Zeeuw, D. L. (2010, August). Periodic plasma escape from the mass-loaded Kronian magnetosphere. *Journal of Geophysical Research: Space Physics*, *115*(A08208). Retrieved 2019-03-15, from http://doi.wiley.com/10.1029/2009JA014951 doi: 10.1029/2009JA014951